Electronic Journal of Biotechnology 79 (2026) 100703

Contents lists available at ScienceDirect

Electronic Journal of Biotechnology

journal homepage: www.elsevier.com/locate/ejbt

Research article

Metabolites of native actinomycetes from Sof Umer cave reveal potent antimicrobial activity against selected pathogens in mice infection models ☆

Ebisa Chaluma Abdeta [a,b], Abu Feyisa Meka [a,c], Daniel Girma Hordofa [a,d], Belete Ketema Sime [a,b], Gadisa Abdisa Akkewak [e], Jemal Ali Mahdi [f], Musin Kelel Abas [a,g], Mesfin Tafesse Gemeda [a,g,*]

[a] Biotechnology Department, Addis Ababa Science and Technology University, Addis Ababa, P.O. Box 1647, Addis Ababa, Ethiopia
[b] Department of Biotechnology, Werabe University, Werabe, SNNPR, Ethiopia
[c] Biology Department, Bule Hora University, Bule Hora, Ethiopia
[d] Department of Biotechnology, Wolaita Sodo University, Wolaita Sodo, Ethiopia
[e] Department of Biotechnology, Dambi Dollo University, Dambi Dollo, Ethiopia
[f] Department of Biotechnology, University of Gondar, Gondar, Ethiopia
[g] Bioprocess and Biotechnology Center of Excellence, Addis Ababa Science and Technology University, Addis Ababa, Addis Ababa, Ethiopia

GRAPHICAL ABSTRACT

Metabolites of native actinomycetes from Sof Umer cave reveal potent antimicrobial activity against selected pathogens in mice infection models

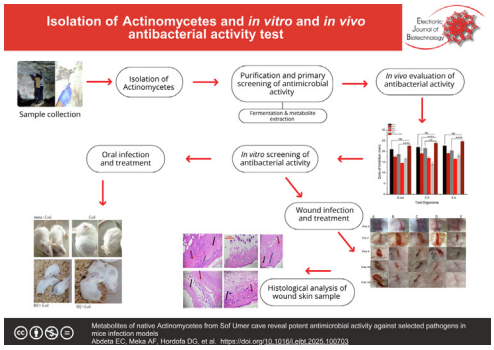

ARTICLE INFO

Article history:
Received 14 July 2025
Accepted 3 September 2025
Available online 13 December 2025

Keywords:
Actinobacterium
Actinomycetes
Antimicrobial activity

ABSTRACT

Background: Actinomycetes are gram-positive bacteria that belong to the actinobacterial species. They are a prolific source of secondary metabolites with various biological applications. Thus, this study aimed to culture-based isolation of potent Actinomycete species from Sof-Umer Cave and *in vitro* and *in vivo* evaluation of their potential metabolites against selected test organisms.
Result: Among the total isolates, ten isolates were selected based on their antimicrobial activities. Among them, the ethyl acetate crude extract of three isolates (RO13, SD2, R011) showed potential antagonistic activity, ranging from 17 ± 0.78 to 23 ± 0.56 mm of zone of inhibition against *Escherichia coli*, *Pseudomonas aeruginosa*, and *Staphylococcus aureus.* Additionally, two isolates' (SD2, R011) crude extract exhibited

Abbreviations: ArcGIS, Architect Geographic Information System; ANOVA, Analysis of Variance; ATCC, American Type Culture Collection; CFU, Colony Forming Unit; DMSO, Dimethylsulfoxide; EPHI, Ethiopian Public Health Institute; FTIR, Fourier Transform Infrared Spectroscopy; GC MS, Gas Chromatography-Mass Spectrometry; ISP2, International Streptomyces Project-2; MHz, Megahertz; MHA, Muller Hinton Agar; NIST MS, National Institute of Standards and Technology Mass Spectrometry; SCA, Starch Casien Agar.

☆ Audio abstract available in Supplementary material.

Peer review under responsibility of Pontificia Universidad Católica de Valparaíso.

* Corresponding author.
E-mail address: mesfin.tafesse@aastuu.edu.et (M.T. Gemeda).

https://doi.org/10.1016/j.ejbt.2025.100703

Arthrobacter sp.
Drug development
Metabolites
Mice infection models
Secondary metabolites
Sof Umer Cave
Streptomycetes flavoviridis

significant inhibition of test organisms in wound and oral infection of the mice models. This was confirmed by wound contraction and progress improvement of the clinical sign observed before treatment. Characterization of their crude extract by FTIR and GC–MS revealed the presence of various functional groups and compounds. Specifically, potent antimicrobial and antioxidant bioactive compounds, such as pyrrolo[1,2-a]pyrazine-1,4-dione, hexahydro-2-piperidine, phenol, 2-methoxy-4-(1-propenyl)-, and indolizine, were identified via GC–MS analysis. Three of the ten potent isolates (R013, R011, and SD2) were identified based on the 16S rRNA gene sequence, and the R013 isolate belongs to *Streptomycetes flavoviridis*, whereas SD2 and R011 were identified as *Arthrobacter* sp. and *Actinobacterium kmd_152*, respectively.

Conclusions: Sof-Umer cave-dwelling actinomycetes possess potent metabolites against test organisms that can be a base for future potent drug development against microbial infections.

How to cite: Abdeta EC, Meka AF, Hordofa DG, et al. Metabolites of native actinomycetes from Sof Umer cave reveal potent antimicrobial activity against selected pathogens in mice infection models. Electron J Biotechnol 2026;79. https://doi.org/10.1016/j.ejbt.2025.100703.

1. Introduction

Actinomycetes are filamentous and spore-forming gram-positive bacteria that belong to the actinobacterial species. Their genetic material contains a high percentage composition of guanine-cytosine (GC) nitrogen bases, typically over 55%, which enables them to survive in various environments [1]. They are metabolically, morphologically, and physiologically highly diverse. Actinomycetes are cosmopolitan and dwell in different environments, including terrestrial, marine, rhizosphere, and extreme environments [2]. Among microbes, Actinomycetes hold primary positions as a source of prolific secondary metabolites. They have been explored widely for their potential to produce various metabolites in antibiotics development [3]. Among the commercially available antibiotics, 70–80% are developed from Actinomycete metabolites [4]. They are also studied as a source of various metabolites for the green synthesis of nanoparticles for various biological applications, particularly *Streptomycetes* spp. [5,6]. The *Streptomyces* genus of Actinomycetes is positioned first with more than 7600 bioactive secondary metabolites, followed by *Nocardia* and *Micromonospora*. However, the genus of Actinomycetes has the genetic potential to produce 10 to 20 bioactive secondary metabolites [7].

Recently, the escalation of antimicrobial-resistant infections has become a threat to public health. Several multidrug-resistant classes of bacteria are aggravating human health problems. *Enterococcus faecalis, Staphylococcus aureus, Klebsiella pneumoniae, Acinetobacter baumannii, Pseudomonas aeruginosa*, and *Enterobacter* species comprise the acronym ESKAPE, which are known to develop multidrug resistance [5]. Some of these groups of bacteria were also used in this study for antimicrobial evaluation of Actinomycetes isolated from Sof Umer Cave. Additionally, *Escherichia coli* was also used, which is known to be resistant to antibiotics and widely used for antimicrobial activity tests [8]. These multidrug-resistant microbial pathogens necessitate searching for potent metabolites for effective treatment against these pathogens. For the exploration of new potential metabolites, many actinobacterial species were targeted from various environments because of their potential to produce potent antimicrobial metabolites. However, the opportunity to find potent metabolite-producing Actinomycetes is limited by repeatedly exploring similar environments and isolating common species from similar sources, such as soil [3,9].

Unexplored extreme environments, such as caves, may harbor potential microbial species with novel bioactive molecules yet to be discovered. In light of this, Ethiopia is well-known for having a variety of climatic zones and unexplored natural ecosystems that possess potential microbial diversity [9]. Previous studies also revealed the presence of potential antibiotic-producing actinomycetes in the different Ethiopian ecosystems [10]. However, caves remain unexplored, notably Sof-Umer Cave, for microbial study. A Sof-Umer Cave is a naturally formed, spectacular limestone cave through which the Weibe River flows [11]. It is an oligotrophic and stressful environment for the survival of microbes due to various abiotic factors. A previous metagenomic study conducted on Sof-Umer Cave revealed the presence of microbial diversity and the existence of functional gene dynamics for potential metabolite production [12]. However, the culture-based isolation of Sof-Umer Cave-dwelling Actinomycetes has not been studied. Therefore, the current study aimed to culture-based isolation of potent Actinomycete species from Sof-Umer Cave and *in vitro* and *in vivo* investigations of their potential antimicrobial activity against selected reference pathogens.

2. Materials and methods

2.1. Description of study area

The Sof-Umer Cave is a remarkable natural limestone environment located in the east Bale zone of the Oromia region, southeastern Ethiopia. It is known by having a 15.1 km length (Fig. S1A [10]), and the Weibe River flows through its interior. It exhibits a minimum temperature range of 19–21°C and a maximum temperature range of 33–35°C year-round. Sof Umer Cave is characterized by high humidity, influenced by a nearby river, and a lack of natural light. The surrounding soil has a pH ranging from 8 to 8.3, with a sandy texture, and is composed of sedimentary rock [13].

2.2. Sample collection

The samples were collected aseptically into sterilized polyethylene bags from inside the cave in sedimentary and rock forms. A total of 600 g of samples was collected for each sample from 0 to 0.7 cm depth of dark zone, ground, and surface of the cave as depicted in Fig. S1B. The samples were maintained in an icebox, transported to the laboratory, and stored at 4°C for further analysis.

The physicochemical characterization of the samples was performed using flame methods.

2.3. Actinomycete isolation

Actinomycetes were isolated via basic preliminary standard serial dilution. For isolation, starch casein agar nutrient media was obtained from the Microbiology Laboratory of the Biotechnology Department of Addis Ababa Science and Technology University (AASTU). Nalidixic acid (25 μg/ml) and cycloheximide (25 μg/ml) were incorporated to inhibit the cross-contamination of bacteria and fungi, respectively. Following the spreading of serially diluted samples, plates were incubated at 28°C for one week [9]. The colonies showed that Actinomycete morphology was subcultured on ISP2 nutrient media, which was obtained from the Microbiology Laboratory of the Biotechnology Department of AASTU, to isolate a pure Actinomycete colony [14]. The pure colonies were preserved in 25% glycerol for further investigation.

2.4. Primary screening of antimicrobial activity

Preliminary screening of antimicrobial production of isolates was done via the perpendicular streaking method using Mueller-Hinton Agar obtained from the Microbiology Laboratory of the Biotechnology Department of AASTU. Briefly, Actinomycete isolates were streaked along straight lines at the center of Mueller–Hinton Agar and incubated at 28°C for 5 d. Reference organisms, such as *S. aureus* ATCC-25923, *P. aeruginosa* ATCC-27853, and *E. coli* ATCC-25922, were refreshed in nutrient broth by the inoculation of a loopful of test organisms. Their optical density was standardized to 0.5 McFarland, equivalent to a cell density of 10^6–10^8 CFU/mL after incubation for 24 h, using a spectrophotometer at (Biochrom Ltd, Cambridge CB4 OF J, England) 625 nm [15]. The reference organisms were streaked perpendicular to the isolates' colonies and incubated for 24 h at 37°C. The potent isolates were selected based on the inhibition of the test organism.

2.5. Production and extraction of secondary metabolites

Actinomycete isolates that revealed antagonistic activity on at least one test organism were selected for submerged fermentation. Briefly, ISP2 nutrient culture media were prepared, and 200 mL was poured into flasks. Loopful fresh culture isolates were inoculated and incubated in a shaker incubator (ZCZY-CS9, China) at 28°C for 8 d at 150 rpm [4]. After fermentation, the cell-free supernatant and pellets were separated by centrifugation using a centrifuge machine (Cence, China) at 12000 rpm for 20 min at 4°C. The cell-free supernatant was mixed with an equal volume of ethyl acetate (1:1). Ethyl acetate is a moderately polar solvent that can dissolve a wide range of metabolites and low-toxic solvent used for microbial secondary metabolites extraction [16]. A funnel separator (Garg India-India) was used to separate the bioactive compound-containing phases, as depicted in Fig. S2. Finally, the extraction solvent was evaporated at 40°C for 1 h in a vacuum oven (ISO14001, China). The crude bioactive products were collected, measured, and stored at −80°C for bioactivity assays [17].

For intracellular bioactive metabolite extraction, the pellets were sonicated for 16 min at 136 MHz by using an Ultrasonic homogenizer (Athena, India) as depicted in Fig. S3. The sonicated pellets were mixed with equal amounts of ethyl acetate and centrifuged at 5000 rpm for 30 min at 4°C. The supernatants were collected and re-extracted with ethyl acetate three times. The extraction solvent was evaporated at 40°C for 1 h in a vacuum oven (ISO14001, China) [16]. Partially purified bioactive products obtained from intracellular and extracellular sources were assessed separately for their bioactivity.

2.6. In vitro screening of the antimicrobial activity

Antimicrobial activity of ethyl acetate crude extracts of selected isolates was evaluated using the well diffusion method. Briefly, reference organisms, *P. aeruginosa* ATCC-27853, *S aureus* ATCC-25923, and *E. coli* ATCC-25922, were refreshed, and their optical density was adjusted to 0.5 (10^8 CFU/mL) McFarland standard. One hundred microliters of reference organisms were spread separately on sterile Muller–Hinton agar (MHA) plates. The 6 mm well was formed via a borer, and 50 μl of crude extract (100 μg/ml) dissolved in DMSO was loaded into the formed well. Amoxicillin (25 μg/ml) and DMSO obtained from the Microbiology Laboratory of the Biotechnology Department at AASTU were used as positive and negative controls, respectively [9]. After incubation for 24 h, the zone of inhibition was measured, and the potent isolates were selected for *in vivo* evaluation of their antimicrobial activity.

2.6.1. In vivo evaluation of antimicrobial activity by wound infection model

Antimicrobial and wound-healing potency of isolates' crude extract was performed using the protocol described by Köksal Karayildirim et al. [18]. Briefly, the 15 mice, 6 to 8 weeks old and weighing 35 to 40 g, were purchased from the Ethiopian Public Health Institute (EPHI). Mice were acclimatized for one week in polypropylene cages at 23 ± 3°C supplemented with a standard diet and water consisting of a 12 h light/dark cycle with proper care for the animal model according to the "Guide for the Care and Use of Laboratory Animals" published by the Ethiopian Public Health Institution.

Mice were randomly divided into five groups (GI, GII, GIII, GIV, and GV), with each group consisting of three members. Before wound creation, local anesthesia was applied in each group of mice with a dose of ketamine (50 mg/kg body weight), which involved loss of pain sensation in a specific body area around the wound creation site. Then, mice were shaved on their back for wound creation, and the localized dorsal skin of the mice was removed aseptically with the help of a surgical blade. A 1.5 cm long wound was created and refreshed 100 μL volume of 5×10^8 CFU *S. aureus* was applied epicutaneously. The fifth group left without infection was used as a negative control. The treatments were given within 8 h intervals, routinely following observation of infectious signs for 14 d. GI was infected without treatment and was used as the positive control group. Group II was treated with 100 μl of 25 μg/ml amoxicillin. In comparison, Group III and Group IV were treated with 100 μl of 100 μg/ml R011 and SD2 actinomycete isolate-extracted metabolites, respectively, and used as a healing reference.

2.6.2. Recovery of test organism

Mice were sacrificed by cervical dislocation to reduce animal pain and stress. The external wound site was rinsed with 70% alcohol to remove external microbial contaminants to recover the test organism. The internal tissue of the wounded site was removed and placed in sterilized saline water, and vigorously homogenized in Eppendorf tubes. The homogenized suspended sample was serially diluted to a 10^{-3} dilution. One hundred microliters were spread on LB agar (obtained from the Microbiology Laboratory of the Biotechnology Department at AASTU) for each dilution and incubated at 37°C for 24 h. At the end of the incubation period, colonies were counted (30–330 CFU/plate).

2.6.3. Histology examination

Histology analysis of the mice skin tissue samples was done to evaluate the healing potency of the isolates' crude extract. Briefly, 1 cm diameter skin tissue samples were taken from the wounded site of each group of mice and fixed in 4% paraformaldehyde. The samples were dehydrated sequentially with increasing percentages of alcohol, cleaned with xylene, and embedded in paraffin to

obtain paraffin blocks, which were cut into 5 μm pieces. The cut sections were dewaxed by soaking them in xylene overnight. The sample was stained with hematoxylin–eosin to investigate histomorphological changes in the cell and tissue structure due to pathogen infection and the effects of the secondary metabolites of actinomycetes in the case of wound healing by inhibiting infected pathogens. Finally, the skin samples were deparaffinized in xylene and hydrated through a descending alcohol series from 100%. After being stained with hematoxylin, differentiation and rapid bluing steps were performed. Then, the sections dyed with eosin were cleared with fresh xylene, mounted with mounting medium, and observed under a microscope at 20X magnification by covering them with a cover slip [19].

2.6.4. In vivo evaluation of antimicrobial activity by oral infection model

For oral infection and treatments, the *E. coli* ATCC-25922 test organism was refreshed and adjusted to 0.5 (10^8 CFU/mL) McFarland standards. The mice were randomly divided into five groups with three mice per group and designated as GI, GII, GIII, GIV, and GV. Each group was orally infected using oral gavage with 100 μl of *E. coli*, except for GV, which remained uninfected and was used as a negative control.

The mice were monitored for 24 h post-infection for confirmation of infection establishment. Following infectious sign observation, Group I was treated with 100 μl of amoxicillin (25 μg/ml), whereas Groups II and III were treated with 100 μg/ml of the crude R011 and SD2 extracts dissolved in DMSO, respectively. Group IV remained untreated and was used as the positive control, while GV was used as a negative control. The treatment was given continuously for three days with 8 h gaps. The change in body weight, feeding habits, and physical changes were recorded daily. Finally, the mice were sacrificed, and the internal organs, such as the lungs, liver, spleen, stomach, and intestines, were removed. The pathological changes in each organ were observed and recorded [20].

2.7. Molecular identification and characterization

The three most potent isolates (R011, SD22, and R013) were grown on ISP2 media for five days. Their total genomic DNA was extracted via a MarkAll genomic DNA extraction kit. The concentration of extracted genomic DNA was checked using a NanoDrop instrument (Thermo Fisher Scientific – USA). The PCR reaction was performed for 16S rRNA gene amplification using universal bacterial primers 27F (5′-AAACTCAAACGAATTGACGG-3′) and 1492R (3′-TTTGAGTTTGCTTAAGCC-3′). The thermal cycling process was started with an initial denaturation of the target DNA at 95°C for 1 min. This was followed by 25 cycles, including denaturation at 95°C for 20 s, primary annealing at 55°C for 15 s, and primary extension at 72°C for 4 min. The process was completed with a cooling step at 4°C. Finally, PCR amplification was confirmed using agarose gel electrophoresis [14]. The amplified 16S rRNA gene was sequenced, and sequence data were assembled and edited via the Contig Express software version. A comparison of sequence similarity was performed via the NCBI BLASTN https://www.ncbi.nlm.nih.gov/blast. The assembled sequences in FASTA format were submitted to NBCI, and accession numbers were given to each isolate. The sequences were compared with those of in-group and single-group species via MUSCLE via a multiple-sequence alignment program. Finally, the phylogenetic tree was constructed using MEGA X version 7 software.

2.8. Characterization of the isolates' crude extract

2.8.1. Fourier Transform Infrared Spectroscopy (FTIR)

For functional group analysis, isolates' ($R0_{11}$, SD_2, $R0_{13}$) crude extracts were dissolved in ethyl acetate. The dissolved samples were injected into the sample cell. The samples were scanned in the range of 400–4000 cm^{-1} via an FTIR (Nicolet Evolution-300, USA) instrument according to the protocol described by Kalaba et al. [21]. The presence of various functional groups was assessed based on the peak values.

2.8.2. Gas Chromatography-Mass Spectrometry (GC MS) analysis

The volatile bioactive compounds contained in the ethyl acetate crude extract of the actinomycete isolates were analyzed via GC MS (Agilent technology-7890B, USA) employing the protocol described by Rammali et al. [22]. For this analysis, the ethyl acetate crude extract was dissolved in methanol and injected into the column with a 1:4 split mode, with helium used as the carrier gas at a flow rate of 1.7 mL/min. The ion source and quadrupoles were maintained at 230°C and 150°C, respectively. The oven temperature program was initiated at 60°C and completed at 360°C. Data interpretation and compound identification were performed by comparing the obtained mass spectra with data available in the NIST MS 2017 library.

2.9. Data analysis

Statistical data analysis was determined using Image J software and Origin Pro 2018 SR1 version 94 software. One-way analysis of variance (ANOVA) followed by Tukey's honest test was also used.

3. Results

3.1. Sample characterization

Physicochemical characterization of Sof Umer Cave samples showed, it was largely dominated by Magnesium (Mg) with 1016.3 compositions in ppm, Copper (Cu) 209.6, Iron (Fe) 1654.8, Cobalt (Co) 163, and Potassium (K) 225. The detailed content of other minerals in the samples was summarized in the in Table S1.

3.2. Isolation and morphological characterization of actinomycete isolates

A total of thirty-seven actinomycete isolates were selected based on their morphology. Twenty-six colonies from rock samples, designated RO1 to RO26, and eleven colonies from sediment samples, designated SD1 to SD11, as depicted in Fig. S4(A), and other isolates are presented in Fig. S5. For morphological characterization, isolates were cultured on ISP4 for seven days, and the observable characteristics, such as colony size, shape, mycelium formation, and pigments of colonies, were recorded as illustrated in Fig. S4(B) and Table S2. Some isolates were also characterized microscopically using a light microscope (Olympus, China), and their spore, substrate, and aerial mycelium were observed as depicted in the Fig. S6.

3.3. Primary screening of antimicrobial activity

In a preliminary screening of the antimicrobial production, 37 of the total isolates, 10 actinomycete isolates, exhibited antimicrobial activity in at least one reference organism after 24 h of incubation. Specifically, RO1 and SD2 isolates inhibited all test organisms, while others inhibited and retarded one to two growth of test organisms (Fig. S7 and Table S3).

3.4. In vitro screening of antimicrobial activity

Partially purified intracellular and extracellular metabolites of Actinomycete isolates were assessed separately for antimicrobial

activity. However, only the crude extracellular extract of five isolates exhibited inhibitory activity against test organisms. Specifically, R013, R011, and SD2 isolates revealed significant inhibition on both the gram-positive and gram-negative test organisms, comparable to RO5 and RO19. The R011 and SD2 Actinomycete isolates exhibited greater potency and zones of inhibition against *S. aureus and E. coli,* as illustrated in Fig. S8 and Table S4. In the statistical analysis of the inhibition zone, most of the isolates were nonsignificant compared to the positive control of amoxicillin, as depicted in Fig. 1.

3.5. In vivo evaluation of antimicrobial activity in wound infection model

Following wound creation, mice were infected and kept for infectious sign observations as depicted in Fig. S9. The clinical manifestations, such as edema, swelling, skin lesions, redness, pus, and inflammation, were observed at the wound site after 24 h post-infection, as depicted in Fig. 2.

The contraction of the wound size was observed after three days of treatment. However, it became wider for the untreated positive control group, and burst by the 14th day of infection (Fig. 3A, line 3). The treatment groups exhibited varying degrees of wound contraction and the healing process was based on the type of treatment given. The R011 extract-treated and amoxicillin-treated groups presented greater wound contraction and healing processes (Fig. 3B–C, respectively). However, the SD2 extract-treated group (Fig. 3D) still exhibited improved wound contraction and healing processes comparable to a nonmedicated group, as depicted in Fig. 3.

3.5.1. Recovery of S. aureus

The number of recovered test organisms (*S. aureus*) from the positive control group was highly dense and uncountable up to the 10^{-3} dilution factor. However, the treated groups presented a decreased number of recovered colonies, although the extent of the reduction varied based on treatments. The RO11 extract-treated group presented a significant reduction in recovered colonies comparable to the SD2 extract-treated group. The RO11 extract-treated group presented only 2 colonies at the 10^{-2} dilution, while no growth was observed at the 10^{-3} dilution. The SD2 extract-treated group presented uncountable colonies up to the 2-fold dilution, while at 10^{-3}, only 26 colonies were observed. This demonstrated that the potency inhibition of Actinomycete isolates' crude extract of test organism growth. Uniquely, R011 isolates demonstrated a promising inhibition of test organisms comparable to the SD2-treated group, as depicted in Fig. 4.

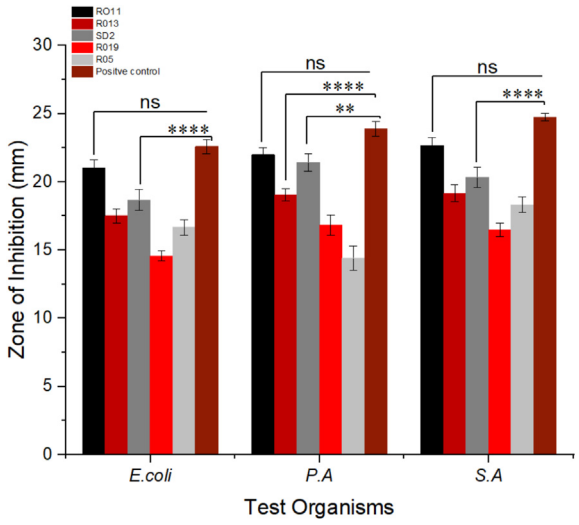

Fig. 1. Graphical representation of secondary antimicrobial screening. * indicates $p < 0.05$, ** indicates $p < 0.01$, *** indicates very significant differences ($p < 0.001$), **** indicates $p < 0.0001$, and ns indicates that, nonsignificant differences.

3.5.2. Histology examination

Histological examination result of negative control skin tissue samples revealed a well-organized structure (Fig. 5B). The epidermis and dermis were properly connected, with a smooth, evenly arranged epidermis. The dermis exhibited a normal distribution of primary skin appendages. However, the positive control samples presented pathological changes containing thickened epidermis, intercellular edema, and blister formation (Fig. 5A). Amoxicillin-treated group presented a good epidermal structure, a properly arranged dermis, and primary skin appendages. However, some less desirable features were also observed, including a non-smooth epidermis, aberrant hair follicles, cell proliferation, and slight edema (Fig. 5C). The R011 extract-treated group presented improved epidermal cell structure and reduced epidermal thickness. However, immune cell proliferation, aberrant hair follicles, and fractured dermal collagen and elastic fibers were observed (Fig. 5D). The SD2 extract-treated group presented with epidermal edema, parakeratosis, and aberrant hair follicles (Fig. 5E). The overall histopathological results for the treated groups revealed significant progress in the healing process comparable to the non-treated group. This finding suggested that the cave isolate actinomycete extract revealed the inhibition of reference organisms and enhanced the wound healing process.

The epidermal thickness of each mouse group was measured as presented in Table S5. Statistical significance between treatments was determined by Tukey's statistical analysis as depicted in Fig. 6.

3.6. Evaluation of antimicrobial activity by oral infection model

Symptoms of infection, such as loss of appetite, rapid heartbeat, changes in body weight, loose hair, bunching, arched back, and semisolid feces, were confirmed after 24 h post-infection in the infected experimental group (Fig. 7).

The observed infectious signs, such as feeding habits and stool condition, significantly improved by the second day of treatment. The body weight of mice was also improved, as provided in Table S6, after two days of treatment. Additionally, physically observed clinical signs, such as rapid heartbeat, hunching, and arched back, were improved in the treated group compared with the untreated group (Fig. 8).

The internal organs of the mice, such as the lung, liver, colon, stomach, and spleen, were examined for pathological changes. The negative control group contained normal intestines with thick, flexible walls, including the lung, liver, colon, stomach, and spleen. However, the positive control group exhibited intestinal congestion, easy rupture, and thinning of the intestinal walls. The intestinal cavity was filled with a yellow viscous liquid, which indicates an abnormality of the intestine. The stomach, lungs, liver, and spleen were also enlarged in size and revealed a color change, while this sign improved for treated groups. The amoxicillin and R011 groups had better effects comparable to the SD2-extract. The SD2 extract-treated group exhibited some alleviation of the clinical signs observed in the positive control. However, the lungs of the SD2-treated group were very large and hemorrhagic, as illustrated in Fig. 9. The alleviation of the physically observable inflammatory response was noted in the treated groups while not for positive control group. Additionally, no organ toxicity was observed as indicated in (Fig. 9), comparable to the crude extract-treated group with negative control.

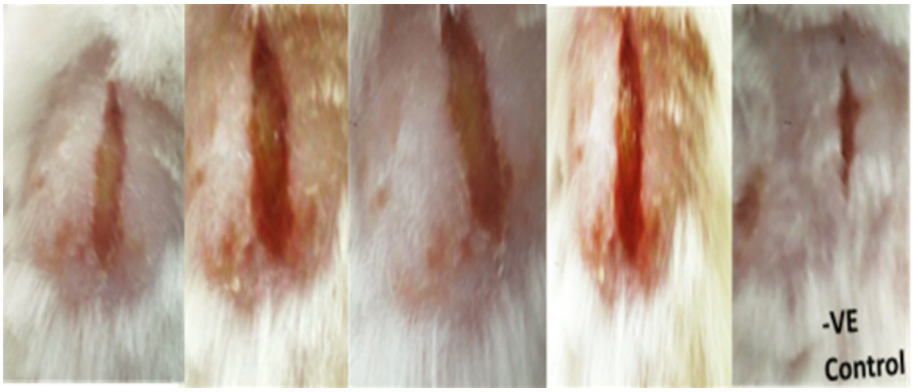

Fig. 2. Symptoms of infection were observed after 24 h post-infection.

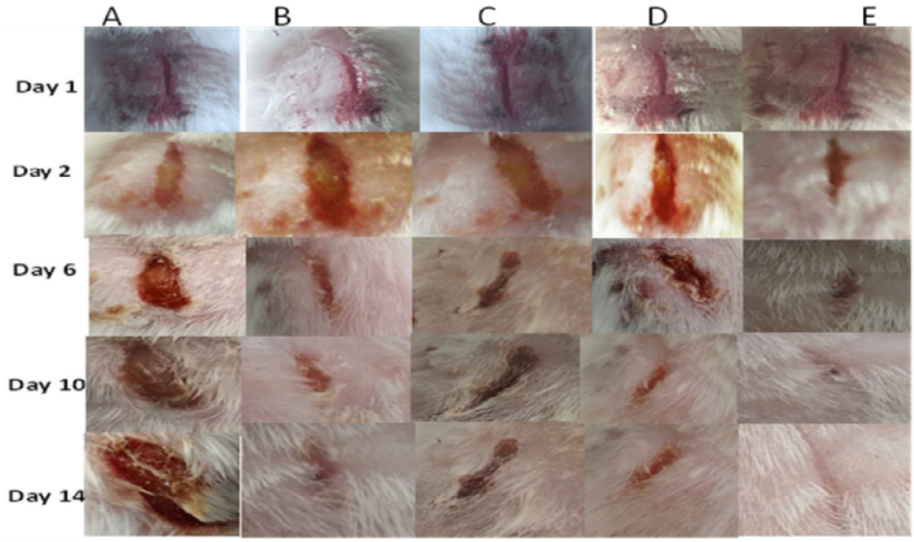

Fig. 3. The representative wound picture was taken on different days. (A) positive control; (B) amoxicillin-treated group; (C) R011 extract-treated group; (D) SD2 extract-treated group; and (E) negative control.

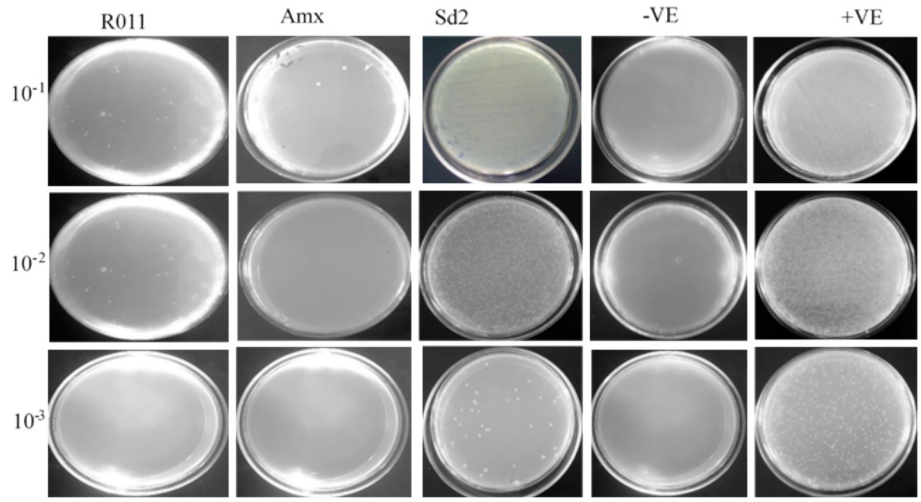

Fig. 4. Recovered the test organism from the wound on the last day. RO11: group mice treated with RO11 isolate's extract, while SD2 is a group treated with SD2 isolate's extract. Amx represents an amoxicillin drug used as the positive control. –ve, for negative control, and +ve for positive control. 10^{-1}, 10^{-2}, and 10^{-3} represent the dilution factor of the sample.

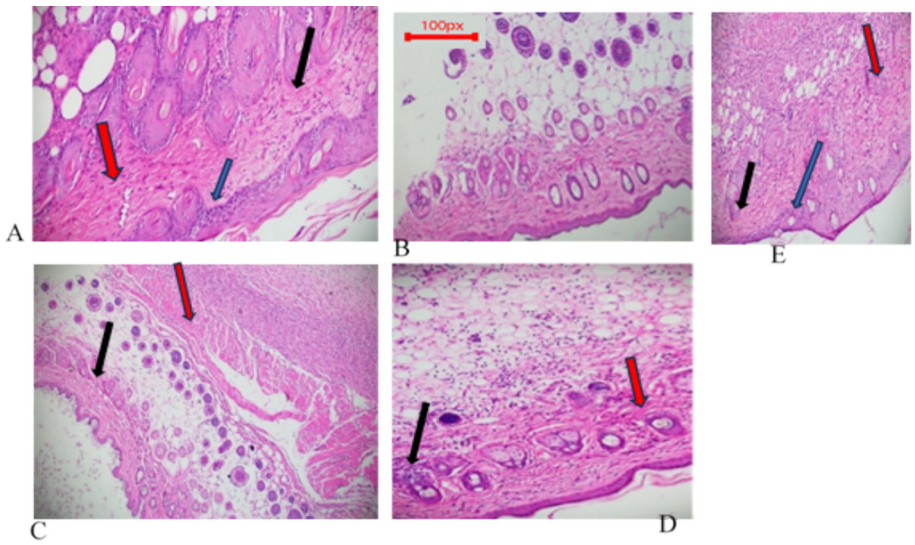

Fig. 5. Histology results under a light microscope at 20X. (A) positive control; (B) negative control; (C) amoxicillin-treated group; (D) R011 extract-treated group; (E) SD2-treated group. Blue arrows indicate parakeratosis and edema, black arrows indicate aberrant hair follicles, and red arrows indicate the proliferation of immune cells. The scale bar indicates the measurement of the epidermal thickness of the skin tissue of mice. (For interpretation of the references to colour in this figure legend, the reader is referred to the web version of this article.)

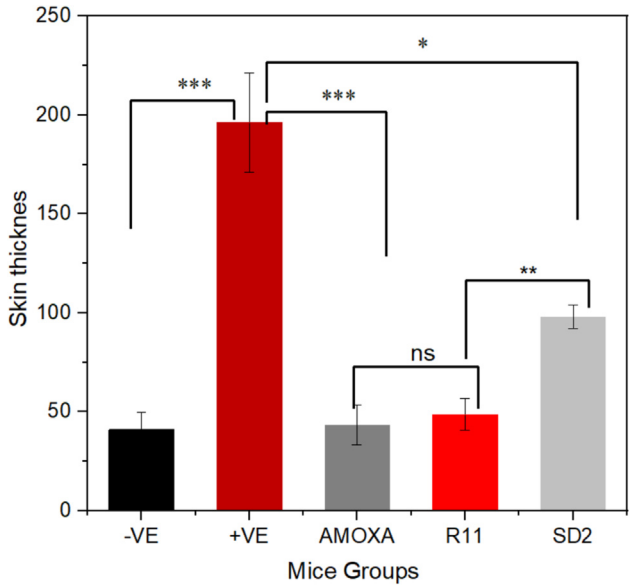

Fig. 6. Measurement of skin sample thickness and statistical significance level between treatments. The streaks indicate statistical analysis between treatments: * indicates $p < 0.05$, ** indicates $p < 0.01$, *** indicates very significant differences ($p < 0.001$), **** indicates $p < 0.0001$, and ns indicates non-significant differences.

3.7. Taxonomic identification of potent isolates

The genomic DNA of three isolates was extracted, and the 16S rRNA gene was amplified by 27F (5′-AAACTCAAACGAATTGACGG-3′) and 1492R (3′-TTTGAGTTTGCTTAAGCC-3′) primers. The amplified gene was visualized by agarose gel-electrophoresis, and about 1200 bp band was formed, as depicted in Fig. S10 and Fig. S11. The sequenced 16S rRNA gene raw data of these isolates were trimmed and aligned via the Contig Express project software. The R013 isolate showed similarity to members of the Streptomyces genus, with 98% homology *S. flavoviridis* strain. A R011 isolate revealed significant similarity to the members of the Actinomycete species, with 99% homology to *the Actinobacterium kmd_152*. SD2 isolate exhibited similarity to the actinobacterial species with 97% homology to *Arthrobacter* sp. *PF3B1*, as revealed in the subsequent phylogenetic tree analysis. These 16S rRNA gene sequence data were submitted to the gene bank to obtain specific accession numbers, and the PQ043200, PQ069280, and PQ056890 accession numbers were given for the SD2, R013, and RO11 isolates, respectively. To reveal their evolutionary relationship, the phylogenetic tree was constructed for isolates using Mega software via the neighbor-joining method, as depicted in Fig. 10.

3.8. Characterization of isolates' crude extract

3.8.1. Fourier Transform Infrared Spectroscopy (FTIR)

FTIR analysis of the ethyl acetate crude extract of the potent isolates presented different peak values as depicted in Fig. 11. The highest peak values were recorded at 3332.896 for the three isolates. This corresponds to O—H stretching vibrations, which are commonly associated with the presence of hydroxyl groups. The 2850–3300 cm^{-1} peak corresponds to C—H stretching vibrations, commonly representing the functional groups of aliphatic or aromatic hydrocarbons. The peak formed from 1680 to 1750 cm^{-1} corresponds to C═O stretching, which commonly represents the carboxyl functional group. The peak formed from 1680 to 1750 cm^{-1} corresponds to C═O stretching, which commonly represents the carboxyl functional group. The functional groups identified under this analysis, such as alkanes, aliphatic, carboxyl, and hydroxyl groups, illustrated the presence of relevant functional groups that can be used as the molecular basis of antibiotic biosynthesis.

3.8.2. Gas Chromatography-Mass Spectrometry (GC MS) analysis

The sixty-three compounds were identified from the R011 extract using GC–MS analysis. The chromatography exhibited different peak values, as depicted in Fig. 12A, representing different compounds. Among the identified compounds, the highest percentage of composition contained compounds presented in Table 1, while the remaining identified compounds were presented in Table S7. SD2 extract analysis presented only sixteen compounds. The chromatography of this isolate presented fewer peak values than the R011 extract, as depicted in Fig. 12B. The major

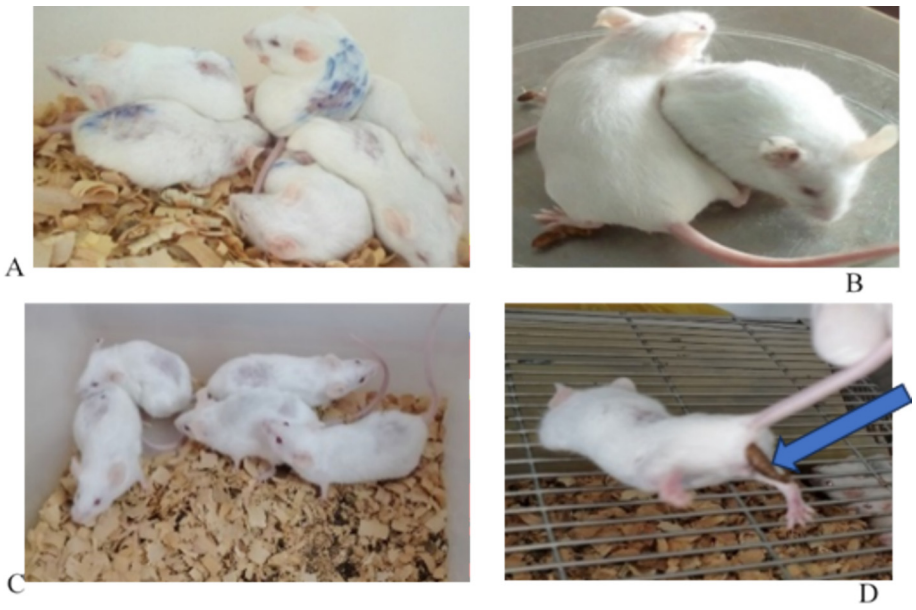

Fig. 7. Observation of clinical signs at 24 h post-infection. (A) infected mice group without treatment; (B) infected and uninfected mice groups together; (C) non-infected control group; (D) change in stool due to infection.

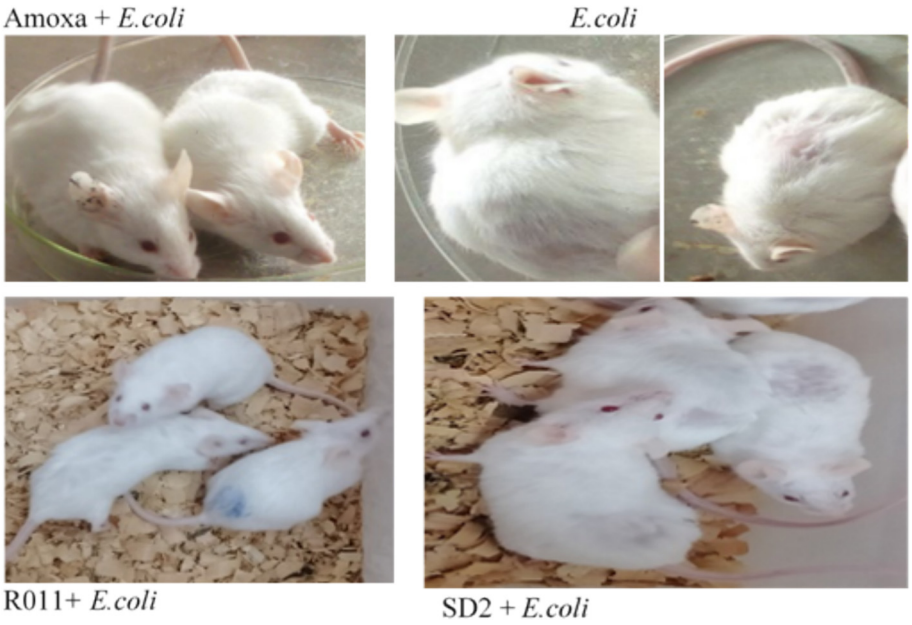

Fig. 8. Photographs were taken after two days of treatment. Amoxa + *E. coli*: infected mice group treated with amoxicillin, as a healing reference. Only the *E. coli* label indicates the infected and untreated mice group. R011 + *E. coli*: infected mice group and treated with R011 isolate's extract, while SD2 + *E. coli* for the infected mice group and treated with SD2 isolate's extract.

compounds based on their percentage of composition are presented in Table 2, while the remaining compounds are presented in Table S8.

4. Discussion

Caves are oligotrophic environments that provide unique stress ecosystems that facilitate microbial interactions. This may lead microbes dwelling in caves to produce potential secondary metabolites to compete with other microbes and conquer available nutrients [23]. However, potential microbial communities in caves are less explored [24], and Actinomycetes are also a large group of Actinobacteria species widely known to inhabit the caves [25]. A number of previous studies conducted on caves also confirmed the existence of a high diversity of cave-dwelling actinomycetes [9,15,17,26]. According to Meka et al. [13], the metagenomic study conducted on Sof-Umer Cave revealed the presence of microbial diversity, including actinobacterial species. The presence of novel functional genes that may be involved in metabolism and the discovery of new bioactive compounds were also reported in this metagenomics study. Thus, the present study attempted to examine the antagonistic activity of Sof Umer Cave-dwelling actinomycetes for selected human pathogen reference organisms.

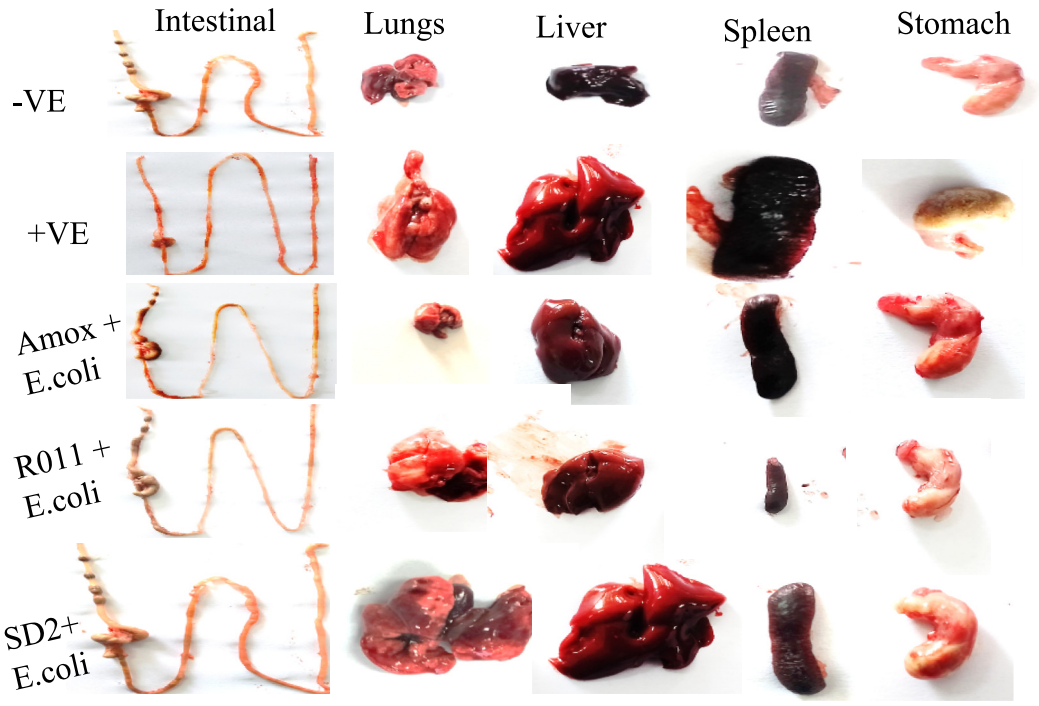

Fig. 9. Internal organs of *E. coli*-infected and non-infected groups of mice. –VE: non-infected organs of mice, +VE: untreated infected control group. Amoxa + *E.coli*: amoxicillin treated infected control group. R011 + *E.coli*: R011 isolate's extract treated group, while SD2 + *E. coli* is for the SD2 isolate's extract treated group.

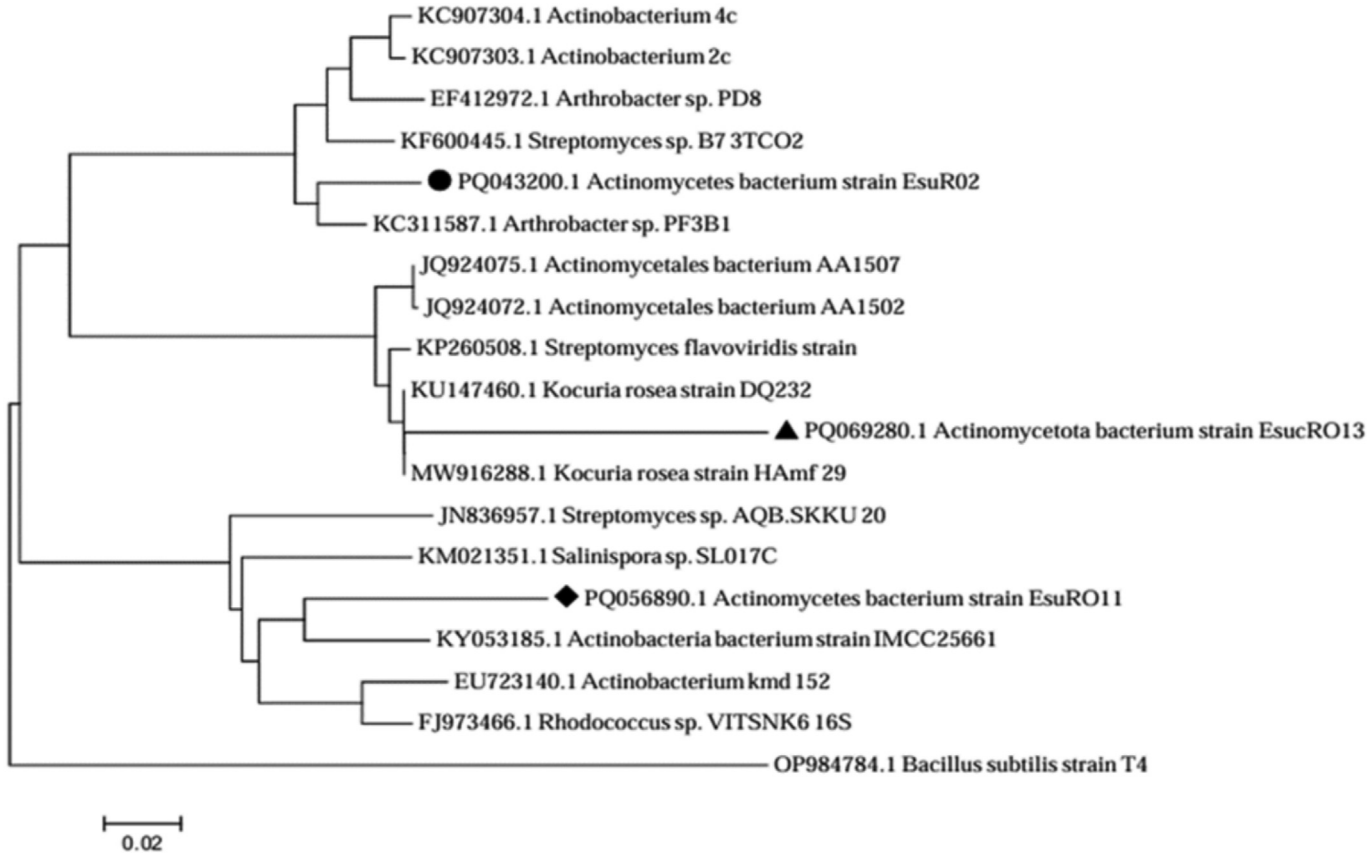

Fig. 10. Phylogenetic tree of three 16S RNA gene sequences of actinomycete isolates. Retrieved from the neighbor-joining analysis showing the evolutionary relationship of isolates SD2 (PQ043200), R011 (PQ069280), and R013 (PQ056890) with their closest BLAST hit. The Bootstrap values (1000 replications) were based on multiple sequence alignment and constructed using the MEGA X version 7 Software.

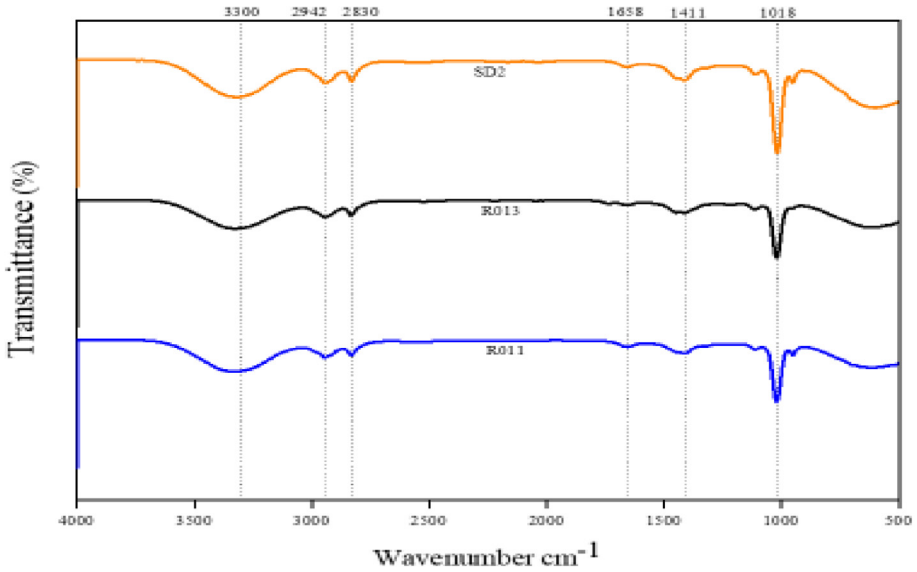

Fig. 11. FTR data analysis of ethyl acetate crude extract of three isolates. The SD2 represents actinomycete isolates from sediments, RO13, and RO11, and Actinomycete isolates from the rock sample.

In our study, most isolates revealed antimicrobial activity against gram-negative in comparison to gram-positive test organisms. However, comparable to our finding, *Streptomyces* spp. isolated from Karst Caves in Türkiye inhibited more Gram-positive (*S. aureus*) than Gram-negative (*E. coli* and *P. aeruginosa*) test organisms [27]. This illustrates the potency of the Sof-Umer Cave actinomycete against more antibiotic-resistant bacteria. Since gram-negative bacteria are known to be more antimicrobial-resistant owing to the unique structure of their cell walls, it provides a permeability barrier that protects them from the penetration of toxic molecule structures [28]. Therefore, this finding paves the way for seeking the best solution for antimicrobial-resistant pathogens. Between the intracellular and extracellular ethyl acetate crude extract of isolates, only the extracellular crude extract exhibited bioactivity against reference organisms, whereas the intracellular metabolites did not reveal any inhibitory activity. This may be due to a specific mechanism of action of extracellular metabolites targeting other environmental microbes for colonization of the niche [29]. *Streptomyces olivaceus* isolated from Shuanghe Cave inhibited *E. coli* and *S. aureus* by 12.5 ± 0.8 and 12.2 ± 0.9 inhibition zone (mm), respectively [23]. However, *S. flavoviridis* and *Actinobacterium kmd_15* isolated from Sof Umer Cave in our study inhibited *E. coli* and *S. aureus* by 17.5 ± 0.78, 21.65 ± 0.7 and 19.25 ± 6, 23 ± 0.56 in mm, respectively. Comparable with this study, the Sof-Umer Cave Actinomycete isolates showed promising antimicrobial activity, which paves the way for exploring potential microbes. Even though the zones of inhibition observed between different studies may not be strictly comparable, this is because the zone of inhibition can be affected by both the effectiveness of the antibiotic and the rate of diffusion through the growth medium [30]. A recent study also reported isolation of *Streptomyces ambofaciens* from Pakistan Cave and ethyl acetate extract of its metabolites presented 25 and 22 mm zones of inhibition for *E. coli* and *S. aureus,* respectively [31]. Comparable to our finding, *Streptomyces* spp. produced a greater zone of inhibition for *E. coli*. However, the zone of inhibition formed by *Streptomyces* spp. in our findings for *S. aureus* was higher than that in this study. Therefore, this finding illustrated that Sof-Umer Cave harbors potential Actinomycete species, which paves the way for the exploration of potent bioactive compounds for the discovery of effective antibiotics from this Cave. The antagonistic activity of isolates is due to the presence of various bioactive metabolites produced by microbes under their optimum growth conditions and the existence of potent microbial metabolites from Caves, as suggested in many previous studies [4,26]. The microbial competition in oligotrophic environments is also another factor influencing the production of potent metabolites for their survival to compete for the available nutrients. This makes Caves fascinating oligotrophic environments for exploring potential microbes for the discovery of novel bioactive compounds [26]. *Streptomyces* spp. are also a potent Actinomycete group that has repeatedly been isolated and known for the production of different potential metabolites reported in different previous studies [5,6], also isolated in this finding, which exhibited potential antimicrobial activity against the reference organism.

The clinical manifestation of the wound infection model occurred as a result of the immune response to *S. aureus* infection [18]. However, in the present finding, actinomycete isolates crude extract presented a great reduction of these clinical signs, wound contraction, and progressive healing. The presence of antimicrobial, ant-oxidant, and anti-inflammatory compounds such as, pyrrolo[1,2-a]pyrazine-1,4-dione, hexahydro-, 2-piperidine, phenol, 2-methoxy-4-(1-propenyl)-, indolizine, cis(+)-3(R,4S)-4-hydroxy-3-(2-nitrosyl), tetrahydro-4H-pyran, phthalic acid and 3,5-dimethyl phenylmethyl ester may contributed to wound contraction and clinical sign alleviation, which were identified via GC MS in the isolates' crude extract. The previous findings also reported that these compounds and their derivatives have bioactivity that inhibits pathogens and is used as anti-inflammatories extracted from various microbes and plants [32,33,34,35,36]. However, further purification and elucidation of their crude extract are indeed relevant in prospective studies to enhance their bioactivity observed in our study for effective antibiotics discovery. An oral *E. coli* infection often causes gastrointestinal discomfort, nausea, and loss of appetite in mice, and reduced food intake leads to a decrease in caloric intake, which results in weight loss [33]. However, actinomycete crude extracts alleviated these clinical symptoms. This may be due to the Sof Umer cave actinomycete producing secondary metabolites that inhibit this test organism. The crude extract of the Sof-Umer Cave Actinomycetes also contained potent antimicrobial, anti-inflammatory, and anticancer bioactive compounds identified by GC MS analysis that contributed to the inhibition of infection in test organisms, which have also been reported by Kavitha and Savithri [35] and Shoaib et al. [36].

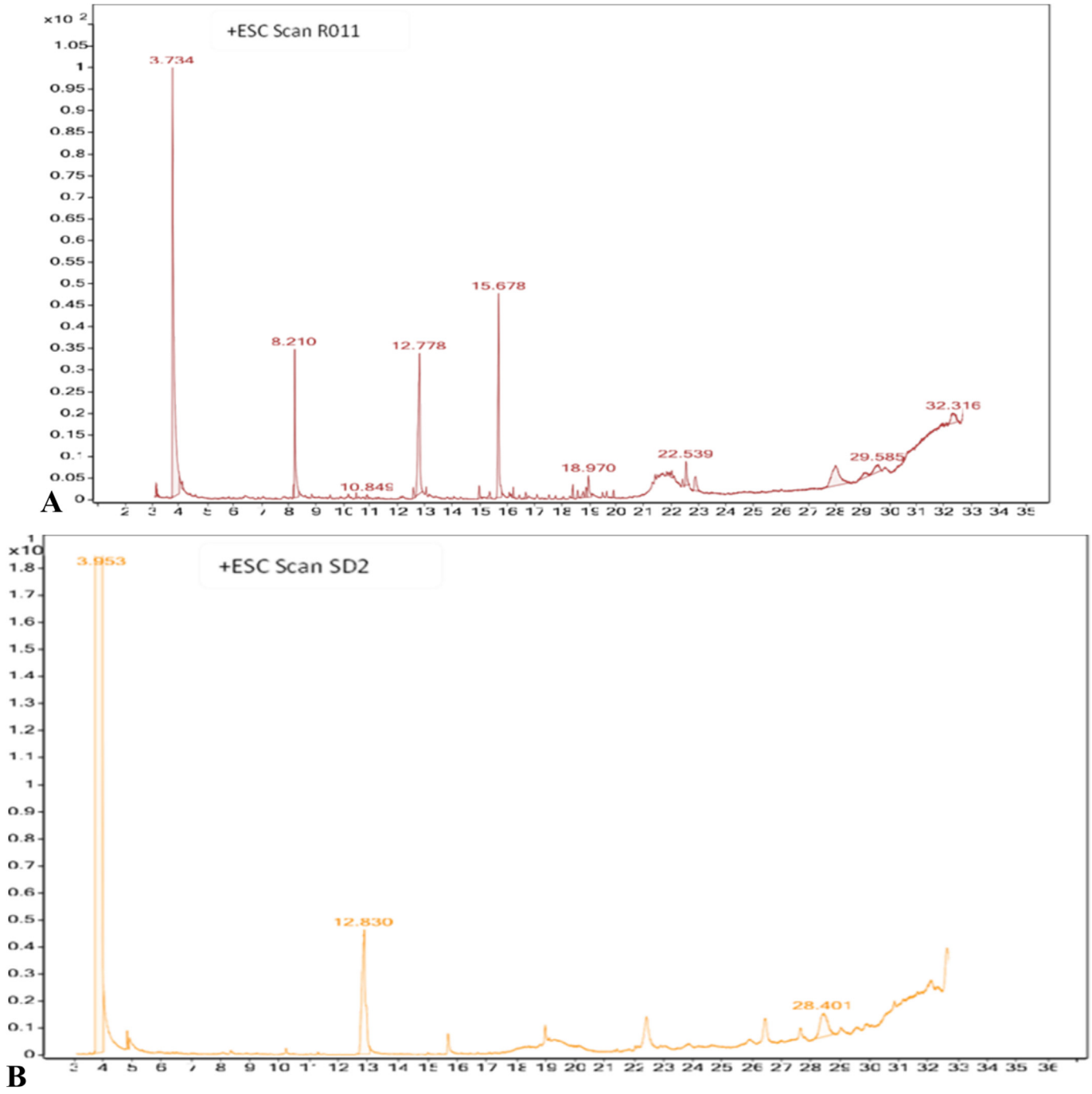

Fig. 12. Chromatographs of GC–MS analysis of Actinomycete isolates. (A) indicates for R011 extract while (B) for SD2 extract.

Particularly, bioactive compounds such as Hexadecanoic acid, methyl ester, as antimicrobial potency [37]. Pyrrolo[1,2-a]pyrazine-1,4-dione, hexahydro-3-(2-methylpropyl as antimicrobial and antifungal [38], and as antimicrobial, anti-inflammatory, antiviral, antifungal, antioxidant, antitumor, and kinase inhibitory [39] are some compounds identified in this study and also reported in a previous study from Actinomycete species. However, further histological analysis of an internal organ of the oral infection mouse models that exhibited physical changes is required for further investigation of the effectiveness of the bioactive compounds of the isolates administered orally.

The FTIR analysis of the ethyl acetate extract of the crude bioactive compounds of Actinomycete isolates presented different functional groups such as aliphatic, ester, hydroxyl, aromatic, alkane, and phenol. The presence of these functional groups may contribute to the different biological applications. In particular, hydroxyl, aliphatic, and phenol functional groups are the main components of many drugs and may contribute to the antimicrobial activity of this study [40]. As reported by Alqahtani et al. [41], almost similar functional groups were identified by FTIR from crude metabolite extract of Actinomycete species isolated from rock soil. From the GC MS analysis, 63 compounds were identified in the *Actinobacterium* sp. (R011) crude extract, whereas 16 compounds were identified in the isolate SD2 (Arthrobacter) extract. The identified compounds contained a versatile group that can be used as antimicrobial, anti-inflammatory, antioxidant, and anticancer agents comparable to previous studies [16,36,42]. These compound groups include organic compounds, alkanes, alkenes,

Table 1
A high percentage composition contained compounds from R011 isolate extract.

No	Compound name	Chemical formula	RT	Area	MW	PC%	Chemical structure	Nature of compound
1	Pyrrolo[1,2-a] pyrazine-1,4-dione, hexahydro-	$C_7H_{10}N_2O_2$	15.678	1,260,911	196.25	14.15480636		Organic compound
2	2-Imidazolidinethione	$C_3H_6N_2S$	12.778	1,254,596	102.168	14.08391508		Organosulfur compound
3	28-Norolean-17-en-3-ol	$C_{29}H_{48}O$	28.002	739,456	410.7	8.301027188		Organic compound
4	2-Piperidinone	C_5H_9NO	8.21	711,672	99.133	7.989127982		Organic compound
5	2,5-Piperazinedione, 3,6-bis(2-methylpropyl)-	$C_{12}H_{22}N_2O_2$	22.539	168,406	226.32	1.890501645	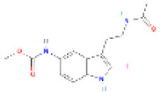	Organic compound
6	Palmitic acid	$C_{16}H_{32}O_2$	18.97	159,118	256.42	1.786235887		Fatty acid
7	Methyl {3-[2-(Acetylamino)ethyl]-2-Iodo-1h-Indol-5-Yl}carbamate	$C_{13}H_{16}N_2O$	22.885	156,375	244.33	1.755443362		Organic compound
8	2,5-Cyclohexadiene-1,4-dione, 2,5-dihydroxy-3-methoxy-6-methyl-	$C_8H_8O_5$	18.877	64,049	140.0936	0.719004904	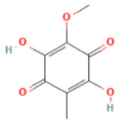	Organic compound
9	3-Isobutylhexahydropyrrolo[1,2-a] pyrazine-1,4-dione	$C_{11}H_{18}N_2O_2$	18.779	46,839	210.27	0.525807908		Organic compound
10	(24R)-Stigmast-5-en-3, beta. –ol	$C_{29}H_5OO$	22.007	45,891	681.2	0.515165796	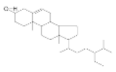	Organic compound

aliphatic compounds, cyclic organic compounds, heterocyclic compounds, lipids, cyclic peptides, aldehydes, and aromatic compounds, which may be one of the reasons for their potential antimicrobial activity. Specifically, pyrrolo[1,2-a]pyrazine-1,4-dione, hexahydro-, 2-piperidine, phenol, 2-methoxy-4-(1-propenyl), and indolizine, which were identified in this study, have also been reported as antimicrobial and antioxidant agents from actinobacterial species [35,43]. The present study focused on the *in vitro* and *in vivo* anti-microbial properties of Sof Umer cave-dwelling actinomycete crude bioactive compounds. Although the Actinomycete crude bioactive extract did not show any specific symptoms in the animal model, investigation of its toxicity is further recommended for future findings. However, this research provides a new view on the potential effects of Sof Umer cave actinomycete crude extracts *in vivo* treatment of mice models infected with test organisms. To the best of our knowledge, this is the first study to provide insight into the *in vivo* bioactivity evaluation of actinomycete crude metabolite extracts on animal models.

5. Conclusions

In conclusion, the Sof Umer Cave Actinomycete species, including *Streptomycetes* sp., *Actinobacterium strain,* and *Arthrobacter* sp., demonstrated promising antagonistic activity in both *in vivo* and *in vitro* tests. The elucidation of their crude culture products confirmed the existence of various compounds and functional groups that may possess wide biological applications. Therefore, this study provides insight into the exploration of actinomycete species from unexplored environments, such as caves, that may harbor potential metabolites that could be useful in addressing the challenges of antimicrobial resistance. Additionally, our findings highlighted Actinomycete strains with their significant potential bioactive com-

Table 2
A high percentage composition contained compounds from SD2 isolate.

No	Compound name	Molecular formula	RT	Area	MW	PC%	Chemical structure	Compound nature
1	Ethylene thiourea	$C_3H_6N_2S$	12.83	2,774,933	102.16	3.179120098	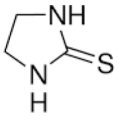	Organosulfur compound
2	Methyl 3-bromo-1-adamantane acetate	$C_{13}H_{19}BrO_2$	28.401	1,101,337	287.19	1.26175392	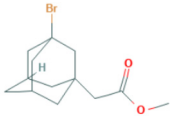	Organic compound
3	Phenol, 2-methoxy-4-(1-propenyl)-	$C_{10}H_{12}O_2$	22.4	755,211	164.2011	0.86521241	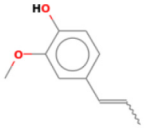	Organic compound
4	Pyrrolo[1,2-a] pyrazine-1,4-dione, hexahydro-	$C_7H_{10}N_2O_2$	15.678	240,915	196.25	0.276005842		Organic compound
5	(24R)-Stigmast-5-en-3. beta.-ol	$C_{29}H_{50}O$	18.964	162,966	681.2	0.186703061	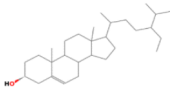	Organic compound
6	(2R,3R,4aR,5S,8aS)-2-Hydroxy-4a,5-dimethyl-3-(prop-1-en-2-yl) octahydronaphthalen-1(2H)-one	$C_{15}H_{24}O_2$	27.627	151,060	236.35	0.173062875	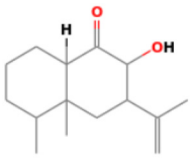	Organic Compound
7	Despropionyl-2-fluorofentanyl	$C_{19}H_{23}FN_2$	23.827	121,777	298.3977	0.139514615	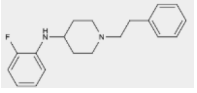	Organic Compound
8	1-(2 Hydroxyethyl)cyclohexane-1,2-diol	$C_8H_{16}O_3$	22.856	93,906	178.27	0.107584022	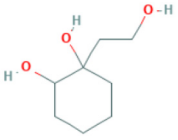	Organic compound
9	Eugenol	$C_{10}H_{12}O_2$	10.179	43,486	164.2	0.04982002	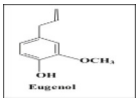	Organic compound
10	Cholest-5-en-3-yl (9Z)-9-octadecenoate	$C_{45}H_{78}O_2$	24.6	38,261	651.1	0.043833964	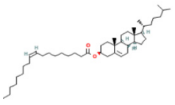	Organic compound

pounds and their applications in pharmaceuticals. *In vivo* and *in vitro* methods were adopted for a comprehensive assessment of their antagonistic activity to determine their potency. However, this study is limited to a small part of the cave, which may not represent the full diversity of actinomycetes inhabiting in Sof Umer cave ecosystem. Additionally, characterization of metabolites and further detailed chemical analyses are indeed relevant for fully understanding their mechanism of action and structures. Therefore, prospective research should emphasize the purification and elucidation of secondary metabolites for developing potential antibiotics.

CRediT authorship contribution statement

Ebisa Chaluma Abdeta: Writing – review & editing, Writing – original draft, Methodology, Investigation. **Abu Feyisa Meka:** Writing – review & editing, Conceptualization. **Daniel Girma Hordofa:** Methodology, Investigation. **Belete Ketema Sime:** Investigation, Data curation. **Gadisa Abdisa Akkewak:** Data curation, Conceptualization. **Jemal Ali Mahdi:** Data curation, Conceptualization. **Musin Kelel Abas:** Visualization, Validation, Supervision, Conceptualization. **Mesfin Tafesse Gemeda:** Writing – review & editing, Visualization, Validation, Supervision, Methodology, Investigation, Conceptualization.

Ethics approval (animals)

All animal-based experiments are performed in line with Addis Ababa Science and Technology institutional animal care and use committee (IACUC) policies and guidelines. The *in vivo* animal model-based studies were designed in consideration of animal rights and welfare guidelines designated in the IACUC that reduce the use of animals.

Financial support

This research did not receive any specific grant from funding agencies in the public, commercial, or not-for-profit sectors.

Declaration of Competing Interest

The authors declare that they have no known competing financial interests or personal relationships that could have appeared to influence the work reported in this paper.

Acknowledgements

The authors acknowledged Addis Ababa Science and Technology University for laboratory facilities.

Supplementary material

https://doi.org/10.1016/j.ejbt.2025.100703.

Data availability

All the data recorded during this study are attached separately as supplementary material as evidence for this research. The sequence data have been deposited in the NCBI database under the following accession numbers: PQ069280, PQ043200, PQ056890.

References

[1] De Simeis D, Serra S. *Actinomycetes*: A never-ending source of bioactive compounds—An overview on antibiotics production. Antibiotics 2021;10(5):483. https://doi.org/10.3390/antibiotics10050483. PMid: 33922100.
[2] Budhathoki S, Shrestha A. Screening of Actinomycetes from soil for antibacterial activity. Nepal J Biotechnol 2020;8(3):102–10. https://doi.org/10.3126/njb.v8i3.33664.
[3] Ganesan P, Reegan AD, David RHA, et al. Antimicrobial activity of some actinomycetes from Western Ghats of Tamil Nadu, India. Alex J Med 2017;53(2):101–10. https://doi.org/10.1016/j.ajme.2016.03.004.
[4] Bhat MP, Nayaka S. Cave soil *Streptomyces* sp. strain YC69 antagonistic to chilli fungal pathogens exhibits *in vitro* anticancer activity against human cervical cancer cells. Appl Biochem Biotechnol 2023;195:6232–55. https://doi.org/10.1007/s12010-023-04388-y. PMid: 36853440.
[5] El-Sherebiny G, Ali ARA, Ali DM, et al. Bioengineering of zinc oxide nanoparticles as therapeutics for immunomodulatory and antimicrobial activities. Egypt J Chem 2022;65(131):1473–86. https://doi.org/10.21608/ejchem.2022.136366.6008.
[6] Kalaba MH, El-Sherbiny GM, Ewais EA, et al. Green synthesis of zinc oxide nanoparticles (ZnO-NPs) by *Streptomyces baarnensis* and its active metabolite (Ka): A promising combination against multidrug-resistant ESKAPE pathogens and cytotoxicity. BMC Microbiol 2024;24:254. https://doi.org/10.1186/s12866-024-03392-4. PMid:38982372.
[7] Busi S, Pattnaik SS. Current status and applications of actinobacteria in the production of anticancerous compounds. In: Singh BP, Gupta VK, Passari AK, editors. New and future developments in microbial biotechnology and bioengineering. p. 137–53. https://doi.org/10.1016/B978-0-444-63994-3.00009-6.
[8] Nyirabahizi E, Tyson GH, Dessai U, et al. Evaluation of *Escherichia coli* as an indicator for antimicrobial resistance in *Salmonella* recovered from the same food or animal ceca samples. Food Control 2020;115:107280. https://doi.org/10.1016/j.foodcont.2020.107280.
[9] Nawaz S, Fatima A, Saleem M, et al. Exploring the antimicrobials production potential of actinobacteria isolated from caves at Bahadurkhel Karak, Pakistan. Proc Pak Acad Sci B Pak Acad Sci Life Environ Sci 2023;60(1):101–12. PMid: 35250404.
[10] Chali K, Belay Z, Bacha K. *In vitro* bioassay of antibacterial and antifungal activity studies of actinomycetes from soda lakes of Ethiopia. Sys Rev Pharm 2022;13(8):798–807. https://doi.org/10.21203/rs.3.rs-668562/v1.
[11] Elias F, Muddada S, Muleta D, et al. Antimicrobial potential of *Streptomyces* spp. isolated from the Rift Valley Regions of Ethiopia. Adv Pharmacol Pharm Sci 2022;2022(1):1724906. https://doi.org/10.1155/2022/1724906.
[12] Asrat A. Geology, geomorphology, geodiversity and geoconservation of the Sof Omar Cave System, Southeastern Ethiopia. J Afr Earth Sc 2015;108:47–63. https://doi.org/10.1016/j.jafrearsci.2015.04.015.
[13] Meka AF, Bekele GK, Abas MK, et al. Exploring microbial diversity and functional gene dynamics associated with the microbiome of Sof Umer cave, Ethiopia. Discov Appl Sci 2024;6:400. https://doi.org/10.1007/s42452-024-06110-x.
[14] Rante H, Manggau MA, Alam G, et al. Isolation and identification of Actinomycetes with antifungal activity from karts ecosystem in Maros-Pangkep, Indonesia. Biodiversitas 2024;25(2):458–64. https://doi.org/10.13057/biodiv/d250203.
[15] Pipite A, Lockhart PJ, McLenachan PA, et al. Isolation, antibacterial screening, and identification of bioactive cave dwelling bacteria in Fiji. Front Microbiol 2022;13:1012867. https://doi.org/10.3389/fmicb.2022.1012867.
[16] Almuhayawi M, Mohamed M, Abdel-Mawgoud M, et al. Bioactive potential of several actinobacteria isolated from microbiologically barely explored desert habitat, Saudi Arabia. Biology 2021;10(3):235. https://doi.org/10.3390/biology10030235.
[17] Gatinho P, Salvador C, Gutierrez-Patricio S, et al. From cultural and natural heritage to a reservoir of biomedicine: Prospection of bioactive compounds produced by bacterial isolates from caves. Int Biodeter Biodegr 2024;190:105773. https://doi.org/10.1016/j.ibiod.2024.105773.
[18] Köksal Karayildirim Ç, Şahiner A, Çalişkan S, et al. Isolation, identification, and antimicrobial evaluation of secondary metabolite from *Serratia marcescens* via an *in vivo* epicutaneous infection model. ACS Omega 2024;9(7):8397–404. https://doi.org/10.1021/acsomega.3c09522.
[19] Abeje BA, Bekele T, Getahun KA, et al. Evaluation of wound healing activity of 80% hydromethanolic crude extract and solvent fractions of the leaves of *Urtica simensis* in mice. J Exp Pharmacol 2022;14:221–41. https://doi.org/10.2147/JEP.S363676.
[20] Zhao X. Antimicrobial peptide MPX alleviates the lethal attack of *Escherichia coli* in mice. Ukr J Vet Agric Sci 2021;4(3):16–21. https://doi.org/10.32718/ujvas4-3.03.
[21] Kalaba MH, El-Sherbiny GM, Darwesh OM, et al. A statistical approach to enhance the productivity of *Streptomyces baarensis* MH-133 for bioactive compounds. Synth Syst Biotechnol 2024;9(2):196–208. https://doi.org/10.1016/j.synbio.2024.01.012.
[22] Rammali S, Rahim A, El Aalaoui M, et al. Antimicrobial potential of *Streptomyces coeruleofuscus* SCJ isolated from microbiologically unexplored garden soil in Northwest Morocco. Sci Rep 2024;14:3359. https://doi.org/10.1038/s41598-024-53801-x.
[23] Long Y, Jiang J, Hu X, et al. Actinobacterial community in Shuanghe Cave using culture-dependent and -independent approaches. World J Microbiol Biotechnol 2019;35:153. https://doi.org/10.1007/s11274-019-2713-y.
[24] Cheeptham N, Sadoway T, Rule D, et al. Cure from the cave: Volcanic cave actinomycetes and their potential in drug discovery. Int J Speleol 2013;42(1):35–47. https://doi.org/10.5038/1827-806X.42.1.5.
[25] Sivalingam P, Hong K, Pote J, et al. Extreme environment *Streptomyces*: Potential sources for new antibacterial and anticancer drug leads? Int J Microbiol 2019;2019(1):5283948. https://doi.org/10.1155/2019/5283948.
[26] Zada S, Sajjad W, Rafiq M, et al. Cave microbes as a potential source of drugs development in the Modern Era. Microb Ecol 2022;84(3):676–87. https://doi.org/10.1007/s00248-021-01889-3.
[27] Tüfekci EF, Uzun Ü, Ertunga NS, et al. Investigation of antimicrobial activities and 16S rRNA sequences of actinomycetes isolated from karst caves in the Eastern Black Sea Region of Türkiye. Kahramanmaraş Sütçü İmam Üniversitesi Tarım ve Doğa Dergisi 2023;26(6):1277–90. https://doi.org/10.18016/ksutarimdoga.vi.1226184.
[28] Breijyeh Z, Jubeh B, Karaman R, et al. Resistance of Gram-Negative bacteria to current antibacterial agents and approaches to resolve it. Molecules 2020;25(6):1340. https://doi.org/10.3390/molecules25061340.
[29] Horak I, Engelbrecht G, Rensburg PJJ, et al. Microbial metabolomics: Essential definitions and the importance of cultivation conditions for utilizing *Bacillus* species as bionematicides. J Appl Microbiol 2019;127(2):326–43. https://doi.org/10.1111/jam.14218.
[30] Hossain TJ. Methods for screening and evaluation of antimicrobial activity: A review of protocols, advantages, and limitations. Eur J Microbiol Immunol 2024;14(2):97–115. https://doi.org/10.1556/1886.2024.00035.
[31] Nawaz S, Skala L, Amin M, et al. Genomic, molecular networking–based metabolomic, and bioactivity profiling of actinobacteria from undisturbed caves in Pakistan. Appl Biochem Biotechnol 2025;197:2667–80. https://doi.org/10.1007/s12010-024-05158-0.
[32] Almalki FA. An overview of structure-based activity outcomes of pyran derivatives against Alzheimer's disease. Saudi Pharm J 2023;31(6):998–1018. https://doi.org/10.1016/j.jsps.2023.04.030.
[33] Abeer F-A-R, Mohanad JK, Imad HH, et al. Determination of bioactive chemical composition of methanolic leaves extract of *Sinapis arvensis* using GC-MS technique. Int J Toxicol Pharmacol Res 2017;9(2):163–78.
[34] Hillman PF, Lee C, Nam S-J. Microbial natural products with wound-healing properties. Processes 2022;11(1):30. https://doi.org/10.3390/pr11010030.
[35] Kavitha A, Savithri HS. Biological significance of marine actinobacteria of East Coast of Andhra Pradesh, India. Front Microbiol 2017;8:1201. https://doi.org/10.3389/fmicb.2017.01201.
[36] Shoaib M, Israyilova AA, Ganbarov K. Cyclohexane and its functionally substituted derivatives: Important class of organic compounds with

potential antimicrobial activities. J Microb Biotech Food Sci 2019;9(1):84–7. https://doi.org/10.15414/jmbfs.2019.9.1.84-87.
[37] Elsayed TR, Galil DF, Sedik MZ, et al. Antimicrobial and anticancer activities of actinomycetes isolated from Egyptian soils. Int J Curr Microbiol App Sci 2020;9 (9):1689–700. https://doi.org/10.20546/ijcmas.2020.909.209.
[38] Kumari N, Menghani E, Mithal R. GC-MS analysis of compounds extracted from actinomycetes AIA6 isolates and study of its antimicrobial efficacy. Indian J Chem Technol 2019;26:362–70.
[39] Dehnavi F, Alizadeh SR, Ebrahimzadeh MA. Pyrrolopyrazine derivatives: Synthetic approaches and biological activities. Med Chem Res 2021;30:1981–2006. https://doi.org/10.1007/s00044-021-02792-9.
[40] Miklasińska-Majdanik M, Kępa M, Wojtyczka RD, et al. Phenolic compounds diminish antibiotic resistance of *Staphylococcus aureus* clinical strains. Int J Environ Res Public Health 2018;15(10):2321. https://doi.org/10.3390/ijerph15102321.
[41] Alqahtani SS, Moni SS, Sultan MH, et al. Potential bioactive secondary metabolites of *Actinomycetes* sp. isolated from rocky soils of the heritage village Rijal Alma, Saudi Arabia. Arab J Chem 2022;15:103793. https://doi.org/10.1016/j.arabjc.2022.103793.
[42] Mothana AA, Al-Shamahy HA, Mothana RA, et al. *Streptomyces* sp. 1S1 isolated from Southern coast of the Red Sea as a renewable natural resource of several bioactive compounds. Saudi Pharm J 2022;30(2):162–71. https://doi.org/10.1016/j.jsps.2021.12.012.
[43] Ser H-L, Palanisamy UD, Yin W-F, et al. Presence of antioxidative agent, Pyrrolo [1,2-a]pyrazine-1,4-dione, hexahydro- in newly isolated *Streptomyces mangrovisoli* sp. nov. Front Microbiol 2015;6:854. https://doi.org/10.3389/fmicb.2015.00854.